



Cite this: *Green Chem.*, 2019, **21**, 2801

## Catalytic valorization of the acetate fraction of biomass to aromatics and its integration into the carboxylate platform†

Bartosz Rozmystowicz,<sup>‡a</sup> Jher Hau Yeap,<sup>‡a</sup> Ahmed M. I. Elkhairy,<sup>a</sup> Masoud Talebi Amiri,<sup>a</sup> Robert L. Shahab,<sup>a,b</sup> Ydna M. Questell-Santiago,<sup>a</sup> Charilaos Xiros,<sup>b</sup> Benjamin P. Le Monnier,<sup>a</sup> Michael H. Studer<sup>b</sup> and Jeremy S. Luterbacher<sup>‡\*a</sup>

In many plant species, the acetate fraction is the fourth most prominent fraction by weight after cellulose, hemicellulose and lignin, and can be easily extracted as a single stable molecule, acetic acid, at high yields. Despite this, upgrading the acetate fraction of biomass has received very limited attention. Here, we demonstrate a valorization route for the acetate fraction as well as mixtures of acetic acid and other volatile fatty acids produced from the polysaccharide fraction. Aqueous solutions of acetic acid, including solutions produced during steam explosion pretreatment and subsequently purified can be upgraded at high selectivity to a valuable mixture of aromatics, substituted cycloalkenes and gas olefins in a single step using Cu/ZrO<sub>2</sub>. The catalyst displays remarkable stability despite the presence of acids, water and other biomass-derived impurities. We also show that acetic acid can be further valorized over the same catalyst by converting it in the presence of butanoic acid that was produced in a consolidated bioprocess from the same pretreated wood that was the source of the acetic acid. In this case, the acetic acid rapidly keto-nizes with the butanoic acid and the resulting beta-ketones further condense to form aromatics and cycloalkenes with a higher average carbon number than those produced solely from acetic acid. Overall, our process yields a biomass-derived organic oil consisting of aromatics and cycloalkenes that spontaneously separates from water, can be tuned by varying the incoming mixture of carboxylic acids and has suitable properties for being used as a direct blend with aviation fuel.

Received 9th February 2019,  
Accepted 24th April 2019

DOI: 10.1039/c9gc00513g

rsc.li/greenchem

## Introduction

Lignocellulosic biomass is the most abundant terrestrial source of fixed renewable carbon and, because of this, is receiving increasing attention as a source of sustainable fuels and chemicals. Plants that are classified as lignocellulosic biomass contain ~50–65% polysaccharides and ~10–30% lignin. The polysaccharide fraction is generally composed of about two-

thirds six-carbon sugars (mostly glucose) and one-third five-carbon sugars (mostly xylose). Lignin is a complex polymer composed of phenyl propanoid units. Because of the prominence of the polysaccharide and lignin polymers in biomass, upgrading efforts have largely focused on sugars and phenolic monomers.<sup>1</sup> However, carboxylic acids are also a very attractive target.

Significant amounts of acetate groups are attached to the hemicellulose fraction of biomass bound to xylopyranosyl residues (Fig. 1). Mansfield and co-workers reported that acetate

<sup>a</sup>Laboratory of Sustainable and Catalytic Processing, Institute of Chemical Sciences and Engineering, École Polytechnique Fédérale de Lausanne (EPFL), CH-1015 Lausanne, Switzerland. E-mail: jeremy.luterbacher@epfl.ch

<sup>b</sup>Laboratory of Biofuels and Biochemicals, School of Agricultural, Forest and Food Sciences, Bern University of Applied Sciences (BFH), CH-3052 Zollikofen, Switzerland

†Electronic supplementary information (ESI) available: Chemicals and materials, experimental procedure for catalyst preparation, catalyst characterization, catalytic testing, lower heating value (LHV) estimation, ICP-MS analysis, aviation fuel testing, electron microscopy imaging, production of acetic and butanoic acid from beech wood and purification of acetic and butanoic acid. ESI Fig. S1–S12 and Table S1. See DOI: 10.1039/c9gc00513g

‡ Co-first authors who contributed equally to this work.

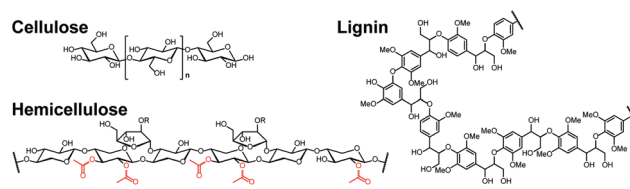


**Fig. 1** Model structures for the three principal lignocellulosic biomass polymers. The acetate fraction (~1–5 wt% of biomass) is highlighted in red.

groups represent between 6.7 and 3.5 wt% of poplar.<sup>2</sup> These acetate groups are much easier to remove from biomass than lignin or polysaccharide monomers. Using relatively mild dilute acid, basic or even neutral conditions, the acetate groups are easily cleaved to produce a single product: acetic acid. This cleavage happens at conditions where only some of the hemicellulose is extracted. Furthermore, unlike lignin monomers<sup>3,4</sup> or sugars,<sup>5,6</sup> acetic acid is stable and does not degrade/re-polymerize making it relatively easy to extract at high yields. Despite the relatively small levels of carboxylic acids in biomass, it represents large amounts of product at the biorefinery scale. Furthermore, acetic acid is often a significant by-product in the carboxylate platform, which consists of converting biomass-derived sugars to a mixture of carboxylic acids. A prominent example of this route is the MixAlco process developed by Holtzapfle and co-workers and where 40–60% of the mixture of carboxylic acids that is produced from biomass is composed of acetic acid.<sup>7–9</sup> Despite the prominence of acetic acid in biomass and various biomass conversion routes, its valorization as a primary biomass-derived platform molecule has received limited attention. Furthermore, the valorization of the acetate fraction of biomass has received almost no attention. Instead, most studies have focused on acetic acid conversion in the context of pyrolysis oil upgrading, where it serves as an attractive model compound for a carboxylic acid group.<sup>10–12</sup> Within this context, a route that is often explored, including in the MixAlco process, is the ketonization of acetic acid to acetone, which allows for the significant removal of oxygen as CO<sub>2</sub> without the need for external hydrogen. Ketonization is typically catalyzed by salts or metal oxides at high temperatures (>300 °C).<sup>9,10,13</sup> Biomass-derived acetone is an attractive substitute for its fossil-derived counterpart but can also be further upgraded. Román-Leshkov and co-workers showed that it could be catalytically upgraded to propylene<sup>14</sup> or isobutene<sup>12</sup> over MoO<sub>3</sub> and zinc-zirconia, respectively. Acetone can also be successively self-condensed over acid and base catalysts first to mesityl oxide and then to mixtures of cyclohexanes and aromatics (e.g. mesitylene, isophorone, etc.) by further condensation and ring closing reactions.<sup>15,16</sup> However, all of these reactions are difficult to perform when starting with aqueous mixtures of acetic acid because the acid and water tend to deactivate catalytic sites that promote ketone deoxygenation or condensation.<sup>14</sup>

Bell and co-workers demonstrated that reactions similar to acetone condensation could occur with a variety of methyl ketones (or beta-ketones) over a base catalyst leading to mixtures of substituted cycloalkanes and aromatic molecules.<sup>17</sup> In their work, the proposed source of beta-ketones is either a hybrid biological and chemical pathway where a mixture of biologically produced acetone, butanol and ethanol (ABE) undergoes acetone alkylation, or deoxygenation and ring opening of carbohydrate-derived furans. In both cases, the associated chemical transformations involve several steps, which limits yields and selectivity to single products.

In this work, we explored the upgrading of an aqueous solution of acetic acid that was easily produced during biomass

pretreatment through combined ketonization and cascade aldol condensation reactions. The objective of combining these two pathways was to produce deoxygenated molecules with a longer carbon chain in a single step for use as a fuel, which has been a significant challenge especially in the presence of water. The jet fuel range (hydrocarbon length from C<sub>8</sub> to C<sub>16</sub>) is a particularly attractive target because it represents a fuel that requires a source of renewable carbon as it cannot be substituted with renewable electricity.

In addition to acetic acid, we also tested an alternate valorization path for acetic acid in the presence of longer chain carboxylic acids, which is a typical mixture associated with the carboxylate platform. We targeted the cross-ketonization of acetic acid with longer chain carboxylic acids (in this case butyric acid produced directly from pretreated biomass) to form beta-ketones, which could condense similarly to acetone.

## Results and discussion

### Proposed reaction pathway

In the process of upgrading short-chain carboxylic acids to potential liquid aviation fuel additives, the carbon chain length must be increased and a significant amount of oxygen removed. Ideally, chain elongation and deoxygenation should occur in a single step. Direct hydrogenation of the carboxylic acids would only result in short gas hydrocarbons. Therefore, we explored conditions that lead to the initial ketonization of the carboxylic acids, and that were conducive to subsequent aldol condensation reactions.

We chose Cu supported on ZrO<sub>2</sub> as the catalyst for carboxylic acid upgrading. As mentioned above, ZrO<sub>2</sub> was previously reported to catalyze the ketonization of carboxylic acids.<sup>10</sup> Separately, it has also been used to perform aldol condensation.<sup>12</sup> The combination of these two reactions could deoxygenate the substrate while increasing the carbon chain length in one step. The addition of Cu served to hydrogenate the longer carbon chain compounds to deoxygenated hydrocarbons and maintain the catalyst's activity by promoting the formation of oxygen vacancies on ZrO<sub>2</sub>. Without Cu, oxygenated compounds adsorbed on the active sites of the catalyst and eventually deactivated it, as observed with experiments using only ZrO<sub>2</sub> (Fig. S1, ESI†). The usage of Cu, which is a relatively mild hydrogenation catalyst, also served to minimize the premature hydrogenation of carboxylic acids. Below, we discuss the potential reaction pathways that occurred on this catalyst for solutions of both pure acetic acid or mixtures of butanoic and acetic acid.

**Reaction pathway of pure acetic acid over Cu/ZrO<sub>2</sub>.** Two acetic acid molecules could ketonize to form acetone (Fig. 2A), losing one molecule of carbon dioxide in the process and reducing the O/C ratio from 1 to 0.33. As the primary intermediate, acetone could react further in two different pathways. Hydrogenation of acetone produced isopropanol, which dehydrated over the metal oxide to form propylene. An alternate pathway was the subsequent aldol condensation of two

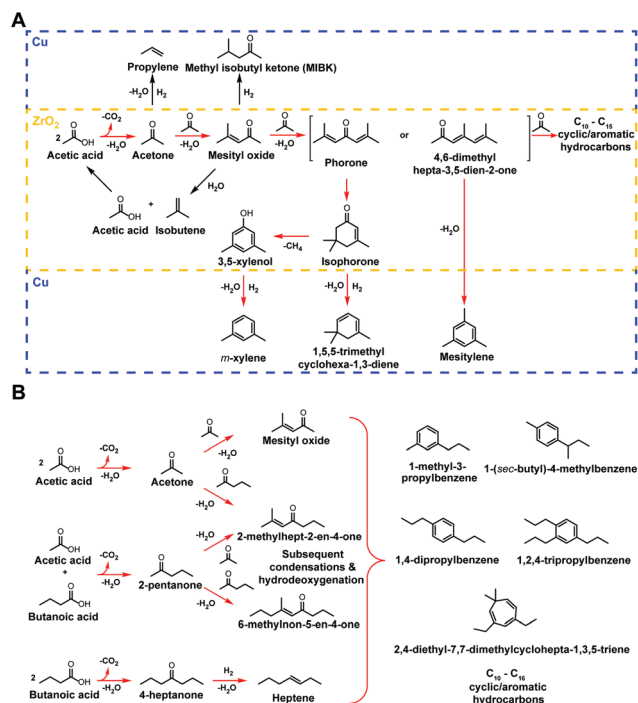


**Fig. 2** Proposed and simplified reaction pathway for the ketonization of carboxylic acids and subsequent cascade aldol condensation reactions to form aromatic hydrocarbons with high carbon numbers. (A) Starting with pure acetic acid and performing direct ketonization. Catalytic sites are highlighted in blue and yellow. The main pathway is highlighted in red. (B) Starting with a mixture of acetic and butanoic acid and performing primarily cross-ketonization. The catalytic sites are not highlighted for simplicity.

acetone molecules to form mesityl oxide. This step lengthened the carbon chain length to six carbons. Further cascade aldol condensations produced products with higher carbon numbers ( $C_9$  to  $C_{15}$ ). Once the carbon backbone exceeded six carbons, intramolecular condensations/ring-closing reactions began to play a significant role forming aromatics and cycloalkenes. For instance, phorone or 4,6-dimethylhepta-3,5-dien-2-one ( $C_9$ ) could undergo ring-closing to form isophorone and intramolecular condensation to form mesitylene, respectively. Importantly, although Cu is a mild hydrogenation catalyst, some hydrogenation could still occur at all steps. A small proportion of acetic acid could be hydrogenated before ketonization and subsequently add to the aldol condensation products, forming a number of compounds with carbon numbers that were not a multiple of three, which could also be formed by decomposition or methane release of higher carbon number compounds ( $C_9$  to  $C_8$  such as isophorone to 3,5-xylene and methane). Cracking reactions could also occur, such as mesityl oxide forming acetic acid and isobutylene. As will be discussed below, through this reaction pathway, the products separated into a triphasic mixture of (i) organic oil formed by a mixture of largely deoxygenated molecules with carbon numbers  $C_8$  to  $C_{15}$ , (ii) an aqueous phase with water formed by deoxygenation reactions or any water in the feed, and unreacted oxygenates

(molecules with at least one oxygen atom), and (iii) gas products consisting of  $CO_2$  and short chain hydrocarbons.

### Reaction pathway of acetic & butanoic acid over Cu/ZrO<sub>2</sub>.

Rather than ketonizing acetic acid with itself, upgrading a mixture of acetic acid and butanoic acid introduced possible cross-ketonization reactions into the reaction pathway (Fig. 2B). Given that mixtures of acetic and longer chain carboxylic acids are commonly produced during the carboxylate platform, such a mixture and reaction scheme could be leveraged to increase the average carbon number of the resulting organic oil. Cross-ketonization proceeded in a similar fashion to direct ketonization, forming  $\beta$ -ketones that could then undergo cascade aldol condensation reactions. Acetone, 2-pentanone and 4-heptanone were potential intermediates, any combination of which could undergo aldol condensation. Similarly, this mechanism also led to a three phase mixture of products, with an organic oil phase containing aromatics and cycloalkenes of higher average carbon number due to the longer chain starting reactants compared to only acetic acid.

### Upgrading of pure acetic acid

We first carried out the upgrading of pure acetic acid as a model feed over 2 g of 2 wt% Cu/ZrO<sub>2</sub> at a weight hourly space velocity (WHSV) of 0.3 h<sup>-1</sup>. As mentioned, the process resulted in a liquid product stream that spontaneously separated into an organic oil phase and an aqueous phase, in addition to a gas stream. Analysis of the molar carbon distribution of all three phases (Fig. 3A) systematically showed complete conversion of acetic acid. The majority of carbons in the liquid phases were present in the form of  $C_8$  and  $C_9$  hydrocarbons. These hydrocarbons primarily consisted of both aromatics (xylenes and mesitylene) and cycloalkenes (dimethyl and trimethyl cyclohexenes). Acetone, the main intermediate in the upgrading route, represented 7.1 mol% carbon of the product stream. Since acetic acid was completely converted but acetone remained, we concluded that the cascade aldol condensation/hydrogenation reactions were rate limiting. In addition, other oxygenates, including ketones and phenols were present in both organic and aqueous phases. Methyl isobutyl ketone (MIBK) was detected, rather than mesityl oxide. The low proportion of MIBK, coupled with no observed mesityl oxide indicated that aldol condensation of products longer than acetone had a higher rate at these reaction conditions compared to hydrogenation.

Over 20 mol% of carbon was converted to  $C_3$  gaseous hydrocarbons, which was likely due to acetone hydrogenation by Cu at these conditions. The ratio of propylene to propane was  $\sim 20$ . Our usage of Cu prevented significant catalyst deactivation, but led to the production of some propylene. However, propylene is a valuable  $\alpha$ -olefin, making it an interesting side reaction. Moreover, the majority of gas hydrocarbons are olefins (including isobutylene, pentene and hexene), with propylene being the predominant product (>50 mol% carbon of total gas). The high ratio of propylene to propane, as well as being the major gas product, should facilitate recovery downstream.

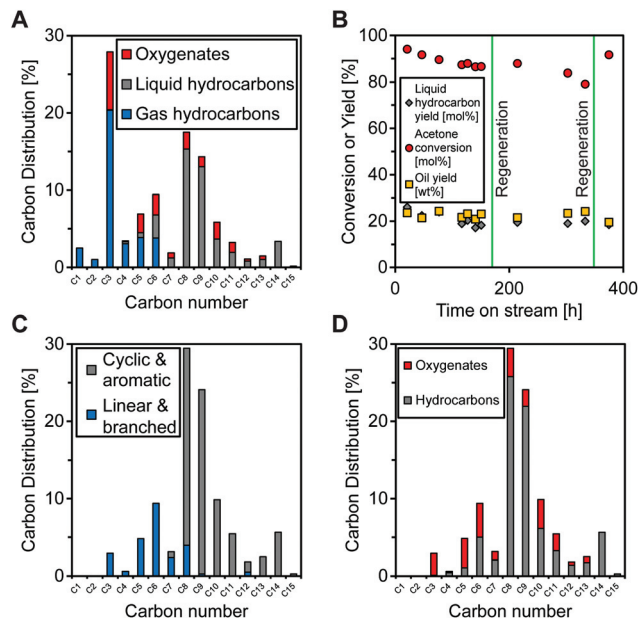


**Fig. 3** Upgrading of pure acetic acid over 2 g 2 wt% Cu/ZrO<sub>2</sub>. (A) Molar carbon distribution of the product stream ( $T = 400\text{ }^{\circ}\text{C}$ ,  $P = 10\text{ bar H}_2$ , WHSV =  $0.3\text{ h}^{-1}$ ,  $\text{H}_2$  flow =  $20\text{ mL min}^{-1}$ , conversion of acetone = 94.2%, time on stream = 21.3 h). Oxygenates consisted of oxygenated molecules in organic, aqueous and gas phases. (B) Acetone conversion, organic oil yield [wt%] and liquid hydrocarbon yield as a function of time. Regeneration of the catalyst carried out at time on stream = 167.6 h and 352.4 h. (C) Molar carbon distribution of linear versus cyclic and aromatic compounds in the organic oil phase (time on stream = 21.3 h). (D) Molar carbon distribution of oxygenates versus hydrocarbons in the organic oil phase (time on stream = 21.3 h).

Interestingly, despite the presence of Cu as a hydrogenation catalyst, the proportion of alkanes and cycloalkanes within the organic oil remained low (1.6 mol% carbon). The prevalence of double bond functionalities was also observed in the gas phase, with propylene being the major product rather than propane. As reducible oxides such as ZrO<sub>2</sub> have high affinity towards bonding oxygenate functionalities, and since the interface between Cu and ZrO<sub>2</sub> is known to be active for hydrogenation,<sup>18</sup> most hydrogenation sites were likely occupied by oxygenates, leading to limited double bond hydrogenation. Similar hydrogenation inhibition behavior with Cu was also observed in our previous work on carboxylic acid upgrading to olefins.<sup>19</sup>

Within the carbon distribution of the product stream, 59.6 mol% were C<sub>6</sub> hydrocarbons or longer, 20.3 mol% was propylene, likely produced through acetone hydrogenation, and 7.1 mol% was unreacted acetone, indicating that the main intermediate was likely acetone and subsequently mesityl oxide. Given the preponderance of aromatic molecules (Fig. S2, S3 and Table S1, ESI<sup>†</sup>), ketonization/cascade aldol condensations was the primary route in the upgrading of acetic acid. To further study the mechanism, we varied the WHSV (Fig. S4, ESI<sup>†</sup>). Increasing the WHSV (*i.e.* decreasing the residence time) increased the proportion of acetone in the

carbon distribution, while the number of products with a higher carbon number decreased. Even at higher WHSVs, acetic acid was not detected. These observations further confirmed that ketonization/cascade aldol condensation was the main reaction pathway, and that ketonization was significantly faster than aldol condensation or hydrogenation reactions, which were the rate limiting steps.

However, the presence of molecules with carbon numbers that were not multiples of three suggests that there are other side reactions happening in addition to these simple cascade reactions. Notably, acetic acid could react in other routes (hydrogenation to acetaldehyde followed by condensation reactions with molecules of a higher carbon number) and higher hydrocarbons could also crack at high temperatures (or release methane from tertiary carbons). These reactions are not necessarily detrimental, as long as the subsequent products have increased carbon chain length. Overall, a mass yield of 23.7 wt% organic oil was obtained at these conditions.

The organic oil mass yield over a course of 150 h time on stream was fairly constant (Fig. 3B), with minor fluctuations probably due to error when handling smaller sample sizes. Because acetic acid was completely converted, we tracked the conversion of the main intermediate, acetone, to characterize the stability of the catalyst. Over 150 h time on stream, the conversion of acetone dropped from 94.2 mol% to 86.7 mol%. However, the combined liquid hydrocarbon and oxygenates yield in the organic oil phase only decreased from 34.8 mol% to 30.8 mol%. The rest of the reduced conversion in acetone was reflected in a loss of propylene yield from 11.9 mol% to 7.4 mol%. Within the organic oil, the yield of liquid hydrocarbons decreased from 26.1 mol% to 18.2 mol%. This indicated that, not only did acetone conversion and organic oil yield slightly decrease because of deactivation on the aldol condensation sites, but the liquid hydrocarbon and propylene yield also slightly decreased due to deactivation of the hydrogenation sites of the catalyst.

Post-reaction characterization (Table 1) of the catalyst showed a slight decrease in copper loading, likely due to inaccuracies in recovering the entire mass of catalyst after reaction. The surface area of the catalyst, total acidity and basicity decreased while the pore size increased. However, the pore volume remained the same. This indicated sintering of the support, which was likely partially responsible for the slight decrease in acetone conversion and organic oil yield. High-

**Table 1** Characterization data for the two catalysts utilized in this study

Catalyst	2 wt% Cu/ZrO <sub>2</sub>	0.5 wt% Cu/ZrO <sub>2</sub>	2 wt% Cu/ZrO <sub>2</sub> (post-reaction)
Cu loading [wt%]	1.74	0.52	1.68
Cu dispersion [%]	7.92	7.00	—
BET surface area [m <sup>2</sup> g <sup>-1</sup> ]	106.97	102.37	30.72
BJH pore size [nm]	3.4	3.4	7.1
BJH pore volume [cm <sup>3</sup> g <sup>-1</sup> ]	0.072	0.081	0.069
Total acidity [μmol g <sup>-1</sup> ]	200	290	92
Total basicity [μmol g <sup>-1</sup> ]	290	296	59

angle annular dark-field scanning transmission electron microscopy (HAADF-STEM) and energy-dispersive X-ray spectroscopy (EDX) mapping of the catalyst (Fig. S5 and S6, ESI†) showed that the catalyst recovered after reaction had some drastically larger copper nanoparticles (30.8–93.0 nm from 3.1–6.9 nm of the fresh catalyst), which demonstrated that some irreversible deactivation was likely due to copper sintering. This particular phenomenon was likely partially responsible for the slight decrease in liquid hydrocarbon and propylene yield.

Regeneration of the catalyst (*via* calcination under synthetic air at 500 °C, followed by reduction under H<sub>2</sub> at 450 °C) restored some of the liquid hydrocarbon yield and acetone conversion, with a second regeneration performing similarly. Overall, the recovery of activity indicated that the deactivation in the first run was partially reversible, with irreversible deactivation likely due to initial copper and pore sintering, followed by reversible coking on the aldol condensation and hydrogenation sites (EDX mapping of the catalyst post-reaction using SiN grids showed small quantities of deposited coke, Fig. S6C and S6D, ESI†).

The carbon distribution of the organic oil phase showed that most compounds were molecules with a carbon number of eight or higher (79.1 mol% carbon) (Fig. 3C). Even though it has six carbons, mesityl oxide only has a five carbon linear backbone, rendering it unlikely undergo intramolecular self-cyclization. This points to the proposed aldol condensation reaction pathway, as the majority of C<sub>6</sub> compounds detected (MIBK) are linear/branched rather than cyclic/aromatic. Overall, 75.1 mol% of the carbon in the organic oil was present as cyclic or aromatic compounds (the molar carbon ratio of monoaromatic to polyaromatic hydrocarbons was 15.3), demonstrating that cyclization was highly favored. Within hydrocarbons in the organic oil that are non-cyclic/aromatic, branched compounds predominate (the molar carbon ratio of branched to linear hydrocarbons was 7).

An analysis of the oxygen content within the organic oil showed that the oil consisted of mostly liquid hydrocarbons (74.9 mol% carbon) rather than oxygenates (Fig. 3D). More importantly, the O/C ratio in the oil was decreased to 0.04, compared to 1 for acetic acid and 0.33 for acetone. This 96% removal of oxygen from acetic acid indicates that our upgrading strategy is viable for producing deoxygenated oil with high carbon numbers. Using the mass fractions of C, H and O within the identified compounds of the oil to estimate the lower heating value (LHV),<sup>20,21</sup> we calculated that the organic oil produced from our process had a LHV of 40.0 MJ kg<sup>-1</sup>. As ASTM D1655 specifications for aviation fuel stipulates a minimum net heat of combustion of 42.8 MJ kg<sup>-1</sup>,<sup>22</sup> our organic oil would not affect the heat of combustion significantly if utilized as a drop-in blend. Additionally, the C<sub>8</sub> to C<sub>15</sub> range of compounds in the organic oil is similar to the carbon number distribution of kerosene-type aviation fuel (C<sub>8</sub>–C<sub>16</sub>).<sup>23</sup> The high aromatic content of the oil (Fig. S7A, ESI†) also makes it suitable for use as an additive for conventional jet fuel (in addition to the high ratio of monoaromatic to polyaromatic hydrocarbons), which influences critical parameters such as lubricity, density and the swelling behaviour of elastomer seals in jet turbines.<sup>24</sup> The presence of phenols in our organic oil could also be beneficial as an antioxidant additive for jet fuel.<sup>22</sup>

matic hydrocarbons), which influences critical parameters such as lubricity, density and the swelling behaviour of elastomer seals in jet turbines.<sup>24</sup> The presence of phenols in our organic oil could also be beneficial as an antioxidant additive for jet fuel.<sup>22</sup>

### Upgrading of dilute & biomass-derived acetic acid

As production of glacial acetic acid is difficult in industrial processes, we explored the use of this process with a diluted acetic acid feed. To this end, we applied this upgrading route for an aqueous feed of 50 wt% acetic acid.

Because aldol condensation is a pseudo-2<sup>nd</sup> order reaction while hydrogenation is a pseudo-1<sup>st</sup> order reaction due to the excess hydrogen that is present in this case, utilization of the same 2 wt% Cu/ZrO<sub>2</sub> catalyst resulted in a large proportion of acetone hydrogenation to propylene (Fig. S8, ESI†). Due to this difference in kinetics, the relative rate of aldol condensation rapidly decreased with decreasing acetone concentrations, compared to hydrogenation. This relative increase in the rate of hydrogenation could be compensated by decreasing the metal loading. Therefore, we used a catalyst for upgrading the dilute acetic acid feed that had a lower copper loading (0.5 wt%) compared to previous experiments (2 wt%).

At these reaction conditions, the conversion of acetone was reduced to 59.2% (Fig. 4A), which was due to the decrease of the aldol condensation rate that accompanied the decrease in reactant concentration with increased water content. The high amount of unreacted acetone further justified the use of a lower copper loading, as a higher copper loading would have preferentially hydrogenated the acetone to C<sub>3</sub> gas hydrocarbons. In this case, the proportion of C<sub>3</sub> gas hydrocarbons (10.6 mol% carbon) was lower compared to 2 wt% Cu/ZrO<sub>2</sub> with pure acetic acid (20.3 mol% carbon), and much lower compared to 2 wt% Cu/ZrO<sub>2</sub> with diluted acetic acid (34.5 mol% carbon). We also performed runs with pure acetic acid with 2 wt% Cu/ZrO<sub>2</sub> and 1 bar H<sub>2</sub> partial pressure (10 vol% H<sub>2</sub> in Ar) which showed similar behaviour (Fig. S9, ESI†), but the catalyst deactivated rapidly, likely due to the insufficient regeneration of oxygen vacancies by molecular hydrogen. The decrease in the aldol condensation rate due to higher water content was also partially mitigated by the increase in total acidity and basicity of 0.5 wt% Cu/ZrO<sub>2</sub> compared to 2 wt% Cu/ZrO<sub>2</sub> (Table 1), as aldol condensation reactions are catalyzed by both acid and basic sites.<sup>10</sup>

Interestingly, the carbon distribution in the liquid phase hydrocarbon mixture shifted from primarily C<sub>8</sub> and C<sub>9</sub> to C<sub>9</sub> and C<sub>10</sub> hydrocarbons, which was also observed with 0.5 wt% Cu/ZrO<sub>2</sub> with pure acetic acid (Fig. S10, ESI†). We attributed this phenomenon to the lower copper loading of the catalyst. Because of the lower hydrogenation rate, more oxygenated molecules underwent aldol condensation reactions to reach higher carbon numbers before being hydrogenated to liquid hydrocarbons. This shift was also observed when a higher WHSV (2.4 h<sup>-1</sup>) was used with 2 wt% Cu/ZrO<sub>2</sub> (Fig. S4, ESI†), where the carbon distribution resembled the results we obtained at 0.5 wt% Cu/ZrO<sub>2</sub>.

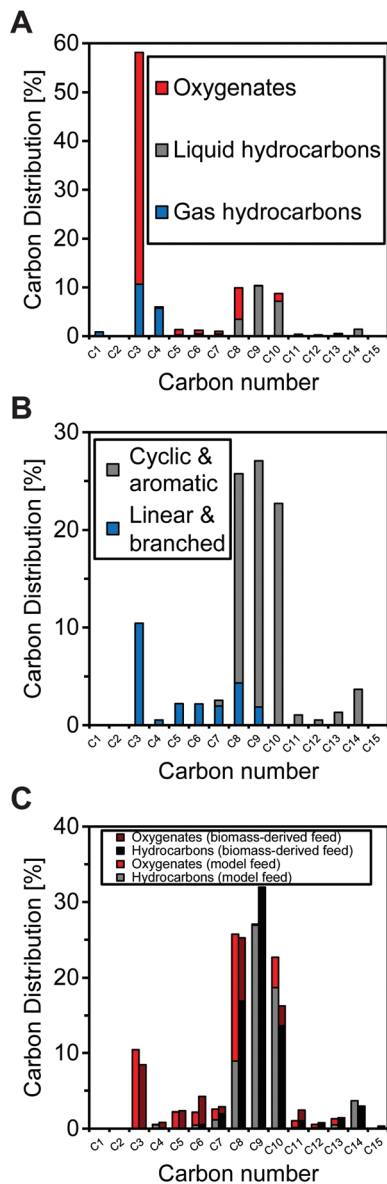


**Fig. 4** Upgrading of 50 wt% aqueous acetic acid over 2 g 0.5 wt% Cu/ZrO<sub>2</sub>. (A) Molar carbon distribution of the product stream ( $T = 400\text{ }^{\circ}\text{C}$ ,  $P = 10\text{ bar H}_2$ ,  $\text{WHSV} = 0.3\text{ h}^{-1}$ ,  $\text{H}_2\text{ flow} = 20\text{ mL min}^{-1}$ , conversion of acetone = 59.2%, time on stream = 265.3 h). Oxygenates consisted of oxygenated molecules in organic, aqueous and gas phases. (B) Molar carbon distribution of linear versus cyclic and aromatic compounds in the organic oil phase (time on stream = 265.3 h). (C) Molar carbon distribution of oxygenates versus hydrocarbons in the organic oil phase for a 50 wt% aqueous acetic acid model feed and 40.3 wt% biomass-derived acetic acid feed (time on stream for model feed = 265.3 h, time on stream for biomass-derived feed = 76.3 h).

As mentioned earlier, at our reaction conditions (with excess hydrogen), hydrogenation likely acted like a pseudo-1<sup>st</sup> order reaction, while aldol condensation acted like a pseudo-2<sup>nd</sup> order reaction. At low acetone conversion, aldol condensation was faster than at higher conversion due to the higher acetone concentration. But as acetone was consumed and the amount of water from condensation increased, the concen-

tration of all substrates (including acetone) decreased, which likely caused the rate of aldol condensation to decrease faster than the rate of hydrogenation. For this reason, at high WHSV (lower acetone conversion), we observed more condensation products vs. hydrogenation products than at lower WHSV. This was also corroborated by the decreased amount of propylene (a product of acetone hydrogenation) at high WHSV. We observed a similar shift to a higher proportion of C<sub>9</sub> and C<sub>10</sub> products with lower H<sub>2</sub> partial pressure, which similarly decreased hydrogenation vs. condensation rates albeit through a different mechanism (Fig. S9, ESI†).

Our analysis of the organic oil phase (Fig. 4B) shows that the majority of carbon was present as cyclic/aromatic C<sub>8</sub>, C<sub>9</sub> and C<sub>10</sub>. Aside from the higher proportion of C<sub>3</sub> linear compounds (mainly acetone) and the increase in C<sub>10</sub>, the rest of the cyclic/aromatic distribution in the organic oil remained similar to reactions with pure acetic acid and 2 wt% copper, with a cyclic/aromatic proportion of 76.5 mol% carbon. Within the organic oil, the molar carbon ratio of monoaromatic to polyaromatic hydrocarbons was 33.9, and branched to linear hydrocarbons was 57.5. The mass yield of the organic oil was 21.2 wt%, and consisted of 61.3 mol% carbon liquid hydrocarbons (Fig. 4C). While this was lower compared to previous experiments, further optimization on the WHSV could increase acetone conversion towards liquid hydrocarbons. Nevertheless, this indicates the possibility of upgrading aqueous acetic acid, which is important for biomass-derived feedstock.

To demonstrate this applicability to real biomass-derived streams, we used the same catalyst and conditions to upgrade 40.3 wt% aqueous acetic acid that was produced from steam-exploded beech wood (see ESI† for detailed separation and concentration protocol). The resulting organic oil had a similar molar carbon distribution (the molar carbon ratio of monoaromatic to polyaromatic hydrocarbons was 37.4, and branched to linear hydrocarbons was 42.1) compared to the reaction with model feed (Fig. 4C), with the only noticeable difference being a small decrease in the yield of C<sub>10</sub> hydrocarbons accompanied by a corresponding increase in the yield of C<sub>9</sub> hydrocarbons. The yield of organic oil was also reduced to 15.4 wt%. Both observations could be due to the increase in the water content of the feedstock, which might have lowered the rate of aldol condensation. Due to limited quantities of biomass-derived acetic acid, the stability of the catalyst was not investigated. However, given the very high purity of the carboxylic acids (aside from water being present) obtained by distillation, we do not anticipate significant catalyst poisoning issues. Overall, these results demonstrated the possibility of upgrading biomass-derived acetic acid produced during pre-treatment to liquid hydrocarbons.

The O/C content of the organic oil was reduced to 0.07 for the model acetic acid feed and 0.06 for the biomass-derived acetic acid feed. This content was slightly higher compared to the 0.04 O/C ratio of the oil from pure acetic acid upgrading, probably due to the decreased rate of hydrogenation as a result of our decision to use a lower copper loading. Nevertheless, this corresponds to a 93% and 94% removal of oxygen from

model and biomass-derived acetic acid, respectively. We similarly estimated the LHV of the organic oil and found 38.3 MJ kg<sup>-1</sup> for model acetic acid and 37.7 MJ kg<sup>-1</sup> from biomass-derived acetic acid. These values are lower compared to the LHV of oil obtained from pure acetic acid, which could be due to the small increase in O/C ratio. Nevertheless, optimization of the reaction conditions could increase the proportion of deoxygenation which would likely increase the LHV of the oil to values similar to those obtained from pure acetic acid. Furthermore, the shift towards carbon numbers of primarily C<sub>9</sub> and C<sub>10</sub> in the upgrading of diluted acetic acid (Fig. S7B and S7C, ESI†) meant that the resulting oil could have a higher distillation curve that would be more comparable with a commercial aviation fuel blending agent.

#### Upgrading of dilute & biomass-derived acetic/butanoic acid mixtures

We also performed cross-ketonization of acetic and butanoic acid to further increase the average carbon number of the organic oil (Fig. 5A). An initial model feed of 28/12 wt% aqueous acetic/butanoic acid feed was used, which corresponded to a 7 : 3 mass ratio of acetic acid to butanoic acid.

Similarly to direct ketonization of acetic acid, full conversion of carboxylic acids was reached. Ketonization products were once again important intermediates, with a large majority of 2-pentanone, which formed most of the oxygenated molecules in the product stream. The significant amount of this product suggested that cross-ketonization was heavily favored compared to homoketonization. This result was obtained with a reduced WHSV of 0.2 h<sup>-1</sup>, because longer chain ketones were slower to condense and required a longer residence time to reach reasonable conversions. As with direct ketonization of acetic acid, compounds in the organic oil that were longer than C<sub>8</sub> were mainly cyclic/aromatic compounds (52.6 mol% carbon) (Fig. 5B). The molar carbon ratio of monoaromatic to polyaromatic hydrocarbons was 85.2, and branched to linear hydrocarbons was 1.4. The decrease in the ratio of branched to linear hydrocarbons could be due to the presence of pentene and heptene in the organic oil, which further indicated the favoring of cross-ketonization (previously with only acetic acid, hydrogenation of the main intermediate acetone produced propylene in the gas phase, rather than pentene in the organic oil, which was produced from pentanone).

The mass yield of the organic oil was 17.8 wt% compared to the original acids in the feed. Within the organic oil phase, 44.5 mol% carbon were liquid hydrocarbons (Fig. 5C). Despite a lower WHSV, the liquid hydrocarbon proportion was still lower compared to direct ketonization of acetic acid, confirming that ketones with a longer carbon chain length had a lower rate of aldol condensation. Because of their increased carbon length, a higher amount of product was retained in the organic oil rather than the aqueous phase. Importantly, liquid hydrocarbons containing eleven carbons or above constitute 12.3 mol% carbon of the organic oil, compared to 4.5 mol% carbon with direct ketonization. This larger fraction of longer carbon chain products demonstrated that cross-ketonization of

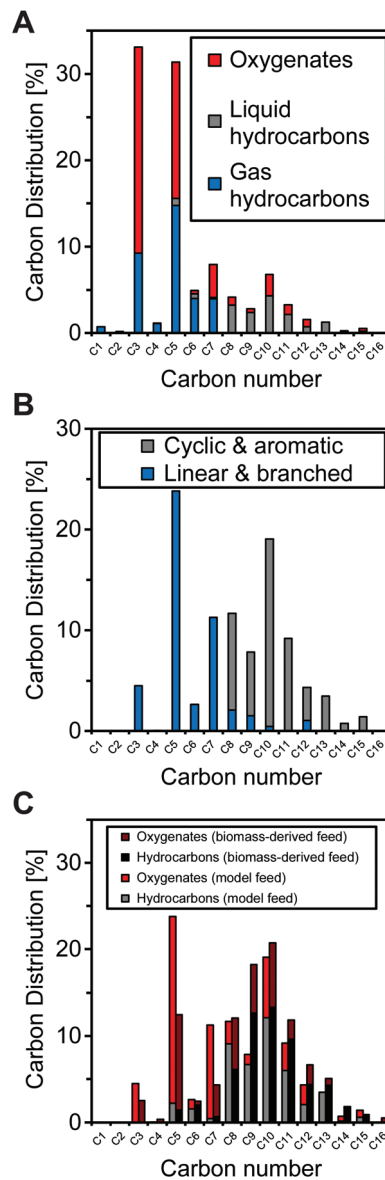


**Fig. 5** Upgrading of 28/12 wt% aqueous acetic/butanoic acid over 3 g 0.5 wt% Cu/ZrO<sub>2</sub>. (A) Molar carbon distribution of the product stream ( $T = 400\text{ }^{\circ}\text{C}$ ,  $P = 10\text{ bar H}_2$ , WHSV = 0.2 h<sup>-1</sup>, H<sub>2</sub> flow = 20 mL min<sup>-1</sup>, time on stream = 72.1 h). Oxygenates consisted of oxygenated molecules in organic, aqueous and gas phases. (B) Molar carbon distribution of linear versus cyclic and aromatic compounds in the organic oil phase (time on stream = 72.1 h). (C) Molar carbon distribution of oxygenates versus hydrocarbons in the organic oil phase for 28/12 wt% aqueous acetic/butanoic acid model feed and 28/12 wt% biomass-derived acetic/butanoic acid (time on stream for model feed = 72.1 h, time on stream for biomass-derived feed = 66.2 h).

acetic acid with butanoic acid can indeed increase the average carbon number of the organic oil, albeit at the expense of total liquid hydrocarbon yield. This chain lengthening showed that the products of the catalytic reactions can be tuned by the properties of the feedstock that is produced biologically.

To demonstrate this concept further, we used this cross-ketonization and aldol condensation platform to upgrade a

mixture of acetic and butanoic acid produced from beech wood. The acetic acid was obtained from steam-explosion of the beech wood, similarly to our experiments above with real acetic acid feeds. After the acetate fraction was removed, the remaining polysaccharides were used to produce butanoic acid in a consolidated bioprocess based on a microbial consortium along with a secondary fermentation (Fig. 6, see ESI† for a description of the process and the subsequent purification). This enabled us to use three fractions of lignocellulosic biomass (cellulose, hemicellulose and acetate) in our upgrading route.

In this case, the oil mass yield was 16.0 wt%, which was similar to the yield obtained when utilizing model feed (Fig. 5C). However, the molar carbon distribution within the organic oil showed a higher proportion of liquid hydrocarbons (57.2 mol% carbon). The molar carbon ratio of monoaromatic to polyaromatic hydrocarbons was 127.6, and branched to linear hydrocarbons was 2.7, which was similar to the model feed. We also measured a comparable amount of liquid hydrocarbons that had a carbon chain length of C<sub>11</sub> or more (21.0 mol% carbon) demonstrating that our catalytic platform can be used to produce a deoxygenated oil from real bio-derived carboxylic acid mixtures.

An analysis of the compounds within the organic oil showed that the O/C content was 0.09 for the model feed and 0.07 for the biomass-derived feed. This compared favorably with the O/C content of oil produced with pure or diluted acetic acid. From the initial O/C ratio of 0.82 (1 for acetic acid and 0.5 for butanoic acid), our upgrading process resulted in an 88% removal of oxygen for the model feed and 91% removal for the biomass-derived feed. LHV estimates indicated a value of 37.5 MJ kg<sup>-1</sup> for the model feed and 38.5 MJ kg<sup>-1</sup> for the biomass-derived feed, similarly to the values estimated for diluted acetic acid feeds. In the case of cross-ketonization, the larger fraction of carbon present as C<sub>11</sub> compounds and above (Fig. S7D and S7E, ESI†) might further benefit the properties of our oil for use as an aviation fuel blending.

### Aviation fuel testing of organic oil as an additive

To demonstrate the viability of the produced organic oil as an additive for aviation fuels, typical aviation fuel parameters were tested for the organic oil produced from pure commercial acetic acid. The process was upscaled to 20 g of 2 wt% Cu/ZrO<sub>2</sub> at the same WHSV of 0.3 h<sup>-1</sup> in order to produce enough

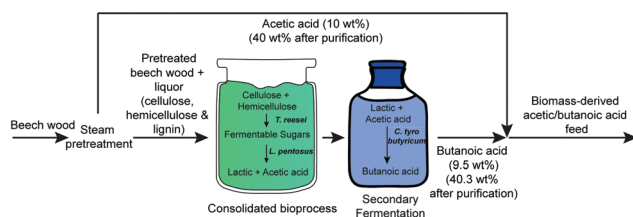


Fig. 6 Steam-explosion of beech wood, followed by consolidated bioprocessing and secondary fermentation of the resulting polysaccharides to obtain biomass-derived acetic and butanoic acid.

Table 2 Aviation fuel testing results for a 10 vol% blend of organic oil with Jet A-1

Property	Test value	Limit <sup>a</sup>	Test method
Aromatics [vol%]	18.3	<25.0	ASTM D1319
Sulfur, total [wt%]	0.032	<0.30	ASTM D5453
Distillation (101.3 kPa)			ASTM D86
Initial boiling point [°C]	64	—	
10 vol% recovered [°C]	165	<205.0	
20 vol% recovered [°C]	171	—	
50 vol% recovered [°C]	189	—	
90 vol% recovered [°C]	230	—	
End point [°C]	267	<300	
Residue [vol%]	0.8	<1.5	
Loss [vol%]	0.2	<1.5	
Density at 15 °C [kg m <sup>-3</sup> ]	801.1	775.0–840.0	ASTM D4052
Specific energy, net [MJ kg <sup>-1</sup> ]	43.2	>42.8	ASTM D3338

<sup>a</sup> As established by AFQRJOS. Limits which do not have a value are only required to report their measured values.

organic oil in a reasonable amount of time. The composition of the organic oil was verified to be similar to the organic oil that was produced at a smaller scale (Fig. S11, ESI†). The purity of the organic oil should be similar to organic oil obtained from biomass-derived acetic acid, as our purification procedure (see ESI† for the procedure) involved distillation of the acids, removing any detectable trace of biomass-derived impurities. Prior to fuel testing, we also performed inductively coupled plasma-mass spectrometry (ICP-MS) measurements on the organic oil, and found metal leaching products such as Cu, Fe and Cr to be below detection limits (Cu and Cr < 0.07 ppm, Fe < 0.68 ppm).

A blend of 10 vol% organic oil with Jet A-1 fuel was tested, in accordance with the test methods of the Aviation Fuel Quality Requirements for Jointly Operated Systems (AFQRJOS): Issue 29 – Oct 2016 for Jet A-1,<sup>25</sup> which encompasses the British Ministry of Defence Standard DEF STAN 91-091/Issue 9 and the ASTM Standard Specification D1655-16a. The test parameters include aromatic content, sulfur content, density, specific energy and the distillation curve (Table 2).

The blended jet fuel had 18.3 vol% aromatics, showing that while the organic oil is composed predominantly of aromatics, it is still suitable to be used as an additive. The sulfur content, density and distillation curve were all within the specifications imposed by AFQRJOS. More importantly, the net specific energy was 43.2 MJ kg<sup>-1</sup>, demonstrating a low oxygen content. Overall, this indicated that our upgrading strategy has the potential to be used for the production of an aviation fuel additive from carboxylic acids.

## Conclusions

In summary, we presented a single step catalytic platform for valorizing the acetate and carboxylate fractions produced from lignocellulosic biomass to jet fuel additives. Model feeds were used initially, which facilitated the identification of the



optimal catalyst and process conditions. We then notably demonstrated that real biomass-derived streams of short-chain carboxylic acids can be upgraded to aromatics and cycloalkenes of eight carbon or higher in a single step. Specifically, aqueous streams of acetic acid and butanoic acid produced from steam pretreatment and subsequently consolidated bioprocessing of the pretreated beech wood were utilized. The resulting organic oil consisted of mainly aromatics and cycloalkenes, with compositions and heating values suitable to be used as additives for aviation fuel, which were further confirmed *via* aviation fuel testing. The results from both model and biomass-derived feed were similar, with minor differences attributed to slight changes in processing conditions (*e.g.* initial water content). Our use of real biomass-derived feed highlights the viability of this platform, as real feeds typically present more challenges (low initial concentrations and biomass related impurities which necessitates concentration and purification) not encountered with model feeds.

Using this method, the valorization of acetate, which is an often neglected fraction of biomass, can contribute to and expand the carboxylate platform that is based on producing carboxylic acids from biomass-derived polysaccharides. Maximizing the use of these different biomass fractions and producing drop in fuels for industries like aviation, where no other sustainable alternatives are currently available, will increase the chances of deploying efficient and profitable biorefineries.

## Conflicts of interest

There are no conflicts to declare.

## Acknowledgements

This work was supported by the Swiss National Science Foundation (SNSF) under the National Research Program 70: Energy Turnaround program (nb: 407040\_153866 and 407040\_153868). This work was also performed in the framework of the Swiss Competence Center for Bioenergy Research (SCCER-BIOSWEET) through the Swiss Commission for Technology and Innovation grant KTI.2014.0116 and by EPFL. We thank Prof. John Ralph (University of Wisconsin – Madison) for discussions on the structure of acetate in lignocellulosic biomass, which were the basis for Fig. 1. We thank the EPFL Central Environmental Laboratory for the ICP-MS analyses.

## Notes and references

- J. S. Luterbacher, D. M. Alonso and J. A. Dumesic, *Green Chem.*, 2014, **16**, 4816–4838.
- A. M. Johnson, H. Kim, J. Ralph and S. D. Mansfield, *Biotechnol. Biofuels*, 2017, **10**, 48.
- L. Shuai, M. T. Amiri, Y. M. Questell-Santiago, F. Héroguel, Y. Li, H. Kim, R. Meilan, C. Chapple, J. Ralph and J. S. Luterbacher, *Science*, 2016, **354**, 329–333.
- L. Shuai, M. Talebi Amiri and J. S. Luterbacher, *Curr. Opin. Green Sustain. Chem.*, 2016, **2**, 59–63.
- S. J. Dee and A. T. Bell, *ChemSusChem*, 2011, **4**, 1166–1173.
- S. K. R. Patil and C. R. F. Lund, *Energy Fuels*, 2011, **25**, 4745–4755.
- P. Thanakoses, A. S. Black and M. T. Holtzappple, *Biotechnol. Bioeng.*, 2003, **83**, 191–200.
- S. Taco Vasquez, J. Dunkleman, S. K. Chaudhuri, A. Bond and M. T. Holtzappple, *Biomass Bioenergy*, 2014, **62**, 138–148.
- M. T. Holtzappple, R. R. Davison, M. K. Ross, S. Aldrett-Lee, M. Nagwani, C.-M. Lee, C. Lee, S. Adelson, W. Kaar, D. Gaskin, H. Shirage, N.-S. Chang, V. S. Chang and M. E. Loescher, *Appl. Biochem. Biotechnol.*, 1999, **79**, 609–631.
- T. N. Pham, T. Sooknoi, S. P. Crossley and D. E. Resasco, *ACS Catal.*, 2013, **3**, 2456–2473.
- T. N. Pham, D. Shi, T. Sooknoi and D. E. Resasco, *J. Catal.*, 2012, **295**, 169–178.
- A. J. Crisci, H. Dou, T. Prasomsri and Y. Román-Leshkov, *ACS Catal.*, 2014, **4**, 4196–4200.
- M. Gliński, J. Kijeński and A. Jakubowski, *Appl. Catal., A*, 1995, **128**, 209–217.
- T. Prasomsri, T. Nimmanwudipong and Y. Román-Leshkov, *Energy Environ. Sci.*, 2013, **6**, 1732–1738.
- F. G. Klein and J. T. Banchemo, *Ind. Eng. Chem.*, 1956, **48**, 1278–1286.
- G. S. Salvapati, K. V. Ramanamurty and M. Janardanarao, *J. Mol. Catal.*, 1989, **54**, 9–30.
- E. R. Sacia, M. Balakrishnan, M. H. Deaner, K. A. Goulas, F. D. Toste and A. T. Bell, *ChemSusChem*, 2015, **8**, 1726–1736.
- I. Ro, Y. Liu, M. R. Ball, D. H. K. Jackson, J. P. Chada, C. Sener, T. F. Kuech, R. J. Madon, G. W. Huber and J. A. Dumesic, *ACS Catal.*, 2016, **6**, 7040–7050.
- J. H. Yeap, F. Héroguel, R. L. Shahab, B. Rozmysłowicz, M. H. Studer and J. S. Luterbacher, *ACS Catal.*, 2018, **8**, 10769–10773.
- S. A. Channiwala and P. P. Parikh, *Fuel*, 2002, **81**, 1051–1063.
- ASTM D4809-18, *Standard Test Method for Heat of Combustion of Liquid Hydrocarbon Fuels by Bomb Calorimeter (Precision Method)*, ASTM International, West Conshohocken, PA, 2018.
- ASTM D1655-18a, *Standard Specification for Aviation Turbine Fuels*, ASTM International, West Conshohocken, PA, 2018.
- G. Hemighaus, T. Boval, J. Bacha, F. Barnes, M. Franklin, L. Gibbs, N. Hogue, J. Jones, D. Lesnini, J. Lind and J. Morris, *Aviation Fuels Technical Review (FTR-3)*, Chevron Products Company, 2007.
- I. A. Al-Nuaimi, M. Bohra, M. Selam, H. A. Choudhury, M. M. El-Halwagi and N. O. Elbashir, *Chem. Eng. Technol.*, 2016, **39**, 2217–2228.
- Aviation Fuel Quality Requirements for Jointly Operated Systems (AFQRJOS): Issue 29 – Oct 2016, Joint Inspection Group (JIG), 2016.